Am J Clin Exp Immunol 2026;15(5):383-397
www.ajcei.us /ISSN:2164-7712/AJCEI0176048

Original Article

Upregulation of KIF18A is associated with poor prognosis and immune alterations in kidney renal papillary cell carcinoma

Wanyu Dong[1], Rong Wei[1], Rushuang Deng[1], Daru Lu[2], Yanqiu Zhang[3]

[1]Department of Hematological Laboratory Science, Jiangsu Key Laboratory of Medical Science and Laboratory Medicine, School of Clinical Medicine and Laboratory Medicine, Jiangsu University, Zhenjiang 212013, Jiangsu, China; [2]State Key Laboratory of Genetics and Development of Complex Phenotypes and MOE Engineering Research Center of Gene Technology, School of Life Sciences, and Taizhou Institute of Health Science, Fudan University, Shanghai 200438, China; [3]SPH XingLing Sci. & Tech. Pharmaceutical Co., Ltd., Shanghai 201707, China

Received August 16, 2026; Accepted October 24, 2026; Epub October 25, 2026; Published October 30, 2026

Abstract: Background: Kidney renal papillary cell carcinoma (KIRP) is a heterogeneous subtype of renal cell carcinoma. Patients with KIRP show variable clinical outcomes. KIF18A is a kinesin-8 motor protein that participates in mitotic chromosome alignment. Previous studies have linked KIF18A to tumor progression. However, its clinical significance and immune relevance in KIRP remain unclear. Methods: RNA-sequencing data and clinicopathological information were obtained from The Cancer Genome Atlas (TCGA). Genotype-Tissue Expression (GTEx) samples were incorporated as additional normal controls when appropriate. We analyzed KIF18A expression, diagnostic performance, survival outcomes, clinicopathological associations, immune infiltration, immune-related genes, differentially expressed genes, and pathway enrichment. Results: KIF18A expression was significantly higher in KIRP tumor tissues than in normal kidney tissues. Receiver operating characteristic analysis showed moderate diagnostic performance, with an AUC of 0.693. High KIF18A expression was associated with shorter overall survival, disease-specific survival, and progression-free interval. It was also related to advanced pathological stage, higher T classification, lymph node involvement, and distant metastasis. Immune infiltration analysis showed that high KIF18A expression was positively associated with T helper cells, Th2 cells, central memory T cells, and activated dendritic cells. In contrast, it was negatively associated with CD8 T cells and cytotoxic cells. Several immune-related genes, including CD200, CD40, CD276, IDO1, ICOS, and PDCD1, were upregulated in the high-KIF18A group. Differential expression analysis identified 1,149 genes, including 896 upregulated genes and 253 downregulated genes. These genes were mainly enriched in cell-cycle regulation, chromosome segregation, mitotic spindle organization, epithelial-mesenchymal transition, and metabolism-related processes. Conclusion: KIF18A is upregulated in KIRP and is associated with poor prognosis, aggressive clinicopathological features, and immune-related alterations. These findings suggest that KIF18A may have prognostic and immune-related relevance in KIRP. Further experimental studies and independent clinical validation are required.

Keywords: Kidney renal papillary cell carcinoma, KIF18A, immune infiltration, immune checkpoint, prognosis, cell cycle

Introduction

Kidney renal papillary cell carcinoma (KIRP) or papillary renal cell carcinoma is a significant histological type of renal cell carcinoma. It exhibits great diversity in molecular characteristics and clinical behavior [1]. The primary curative therapy for localized KIRP is surgery. Nevertheless, there are cases when patients experience recurrence after the operation, metastatic disease progression, or relapse, which may affect long-term results [2-4]. Thus, the discovery of reliable molecular characteristics to risk stratify, assess prognosis, and characterize biology is still a research priority in KIRP [5, 6]. New opportunities have also been opened up by advances in extracellular vesicle isolation and detection of biomarkers to evalu-

https://doi.org/10.62347/JVMV3248

ate disease-related features on a molecular level [7].

Recent research on renal cancer has highlighted the need to understand molecular biomarkers in the tumor microenvironment. In clear cell renal cell carcinoma, cancer-associated fibroblasts play a role in immune evasion, extracellular matrix remodeling, metabolic reprogramming and drug resistance [8, 9]. These findings suggest that stromal and immune elements can have a profound impact on the progression of renal cancer. Genomic analyses of palmitoylation-related genes in clear cell renal cell carcinoma also demonstrate that molecular signatures can help with prognostic stratification and prediction of immunotherapy response [10]. More generally, diagnostic studies based on the tumor microenvironment indicate that combining information about immune, stromal, vascular and other aspects of the tumor microenvironment can enhance the biological understanding and clinical utility of tumor biomarkers [11]. These insights contribute to a holistic view of biomarker studies in kidney cancer.

Dysregulation of the cell cycle and failure in mitotic control are key hallmarks of cancer [12, 13]. Chromosome segregation defects, uncontrolled proliferation and spindle dysfunction can lead to genomic instability and tumor progression [13, 14]. Kinesins are microtubule-based motor proteins that play critical roles in intracellular transport, spindle assembly, chromosome segregation and cytokinesis [15]. KIF18A is a member of the kinesin-8 family. It controls kinetochore-microtubule interactions and ensures proper chromosome alignment during mitosis [16]. As such, KIF18A has been identified as a cancer-associated mitotic protein. Dysregulated KIF18A expression has been found in various cancers, such as renal cell carcinoma and esophageal cancer. Elevated KIF18A expression in these tumors has been linked to increased proliferation, migration, invasion, progression and poor prognosis [17, 18]. Pan-cancer studies also indicate that KIF18A is associated with patient survival and immune-related characteristics in various cancers [19]. Recent functional and pharmacological experiments suggest that chromosomally unstable tumors may be highly dependent on KIF18A-mediated regulation of mitosis. These results support the notion of KIF18A as a potential therapeutic target in this setting [20, 21].

Bioinformatics research also indicates that tumor-associated genes may be prognostic and immunological. For instance, another kinesin family member, KIF15, is a driver in an immunosuppressive microenvironment of breast cancer [22]. This suggests that mitotic motor proteins might play a role not only in cell division but also in immune remodeling. Similarly, TIPARP has been identified as a prognostic and immune-related gene in pancreatic cancer by comprehensive analyses [23]. These approaches offer valuable insights for assessing cancer biomarkers from clinical and immunological aspects. But the function of KIF18A in KIRP is not fully understood. While KIRP has been studied in previous pan-cancer studies, the links between KIF18A and diagnostic accuracy, prognosis, immune features and underlying biological processes have not been thoroughly explored [19]. Thus, a specific analysis of KIF18A may further elucidate the molecular mechanisms underlying KIRP progression and outcomes.

In the current work, we have examined the expression of KIF18A in KIRP through publicly accessible transcriptomic and clinicopathological data. We analyzed its pattern of expression, diagnostic capability, survival correlation, and association with clinicopathologic features. Other factors that were studied included immune infiltration profile, immune regulatory characteristics, and associated biological pathways. These analyses helped us elucidate the possible clinical and biological significance of KIF18A in KIRP.

Materials and methods

Data acquisition and processing

Transcriptomic and clinical data for KIRP and other TCGA cohorts were obtained from The Cancer Genome Atlas (TCGA). For KIRP, STAR workflow-processed RNA-seq TPM data were downloaded from the Genomic Data Commons portal (https://portal.gdc.cancer.gov; accessed 10 June 2026). The TCGA-only comparison included 291 KIRP tumor samples and 32 tumor-adjacent normal samples. To increase the number of normal controls, uniformly processed TPM data for TCGA and Genotype-

Table 1. The abbreviations and corresponding full names of 33 cancers

Abbreviations	Cancer Type
ACC	adrenocortical carcinoma
BLCA	bladder urothelial carcinoma
BRCA	breast invasive carcinoma
CESC	cervical squamous cell carcinoma and endocervical adenocarcinoma
CHOL	cholangiocarcinoma
COAD	colon adenocarcinoma
DLBC	lymphoid neoplasm diffuse large B-cell lymphoma
ESCA	esophageal carcinoma
GBM	glioblastoma multiforme
HNSC	head and neck squamous cell carcinoma
KICH	kidney chromophobe
KIRC	kidney renal clear cell carcinoma
KIRP	kidney renal papillary cell carcinoma
LAML	acute myeloid leukemia
LGG	brain lower grade glioma
LIHC	liver hepatocellular carcinoma
LUAD	lung adenocarcinoma
LUSC	lung squamous cell carcinoma
MESO	mesothelioma
OV	ovarian serous cystadenocarcinoma
PAAD	pancreatic adenocarcinoma
PCPG	pheochromocytoma and paraganglioma
PRAD	prostate adenocarcinoma
READ	rectum adenocarcinoma
SARC	sarcoma
SKCM	skin cutaneous melanoma
STAD	stomach adenocarcinoma
TGCT	testicular germ cell tumors
THCA	thyroid carcinoma
THYM	thymoma
UCEC	uterine corpus endometrial carcinoma
UCS	uterine carcinosarcoma
UVM	uveal melanoma

Tissue Expression (GTEx) were obtained from the UCSC Xena Toil RNA-seq Recompute compendium (https://xenabrowser.net/datapages/) [24, 25]. The integrated analysis included 289 TCGA tumor samples and 60 normal kidney samples, comprising 32 TCGA tumor-adjacent normal samples and 28 GTEx normal kidney samples. Paired analysis included 32 matched tumor-normal pairs.

For TPM-based expression analyses, values were transformed as log2(TPM + 1). The clinical file contained 291 patient-level records. Before patient-level matching, duplicate RNA-seq records were reviewed; for clinical and survival analyses, each patient was represented by a single tumor expression profile. Cases lacking matched expression data or the variables required for a given analysis were excluded as appropriate. No additional batch correction was applied to the Toil-processed TCGA-GTEx data, although residual study-related variation cannot be completely excluded. KIF18A expression was assessed across 33 TCGA cancer types, with the corresponding abbreviations listed in **Table 1**.

Diagnostic and prognostic analysis

The diagnostic and prognostic relevance of KIF18A was assessed by expression-based analyses. Receiver operating characteristic

Table 2. The abbreviations and corresponding full names of 24 immune cell populations

Abbreviations	Immune cell type
aDC	activated dendritic cells
B cells	B lymphocytes
CD8 T cells	$CD8^+$ T lymphocytes
Cytotoxic cells	cytotoxic immune cells
DC	dendritic cells
Eosinophils	eosinophilic granulocytes
iDC	immature dendritic cells
Macrophages	macrophages
Mast cells	mast cells
Neutrophils	neutrophils
NK CD56bright	CD56 bright natural killer cells
NK CD56dim	CD56 dim natural killer cells
NK cells	natural killer cells
pDC	plasmacytoid dendritic cells
T cells	total T lymphocytes
T helper cells	helper T cells
Tcm	central memory T cells
Tem	effector memory T cells
TFH	follicular helper T cells
Th1 cells	type 1 helper T cells
Tgd	gamma-delta T cells
Th17 cells	type 17 helper T cells
Th2 cells	type 2 helper T cells
TReg	regulatory T cells

(ROC) curve analysis was used to evaluate the tissue-level discrimination of KIF18A expression between 291 KIRP tumor samples and 32 tumor-adjacent normal kidney samples in the TCGA cohort. The AUC and 95% CI were estimated using the R package "pROC", and ROC curves were plotted using "ggplot2". Time-dependent ROC analysis was performed using the "timeROC" package, with overall survival as the endpoint, among 290 patients with available OS time and status data; 1-, 3-, and 5-year areas under the curve (AUCs) were calculated [26].

In the pan-cancer analysis, the association between continuous KIF18A expression and overall survival was evaluated using Cox regression, and the results were displayed as forest plots. Kaplan-Meier analyses of overall survival, disease-specific survival, and progression-free interval used endpoint-specific high- and low-expression groups defined using the minimum-*P*-value approach. The R packages "survival" and "survminer" were used for the Kaplan-Meier analyses.

Clinicopathologic correlation analysis

The correlation between the expression of KIF18A and clinicopathological characteristics in KIRP was evaluated by comparing the levels of its expression in various clinical subgroups. The variables that were analyzed were age, gender, pathological stage and TNM classification. The Wilcoxon rank-sum test was used to compare differences between two-category variables, and the Kruskal-Wallis test was used to compare differences between variables with three or more categories.

Immune infiltration and analysis of immune-related genes

KIRP samples were stratified according to KIF18A expression before immune-related analyses were performed. Single-sample gene set enrichment analysis (ssGSEA) was used to estimate the relative infiltration levels of 24 immune cell populations in each sample, and the corresponding immune cell abbreviations are listed in **Table 2** [27, 28]. The correlation between KIF18A expression and patterns of immune infiltration was tested by Spearman correlation analysis. There was also an evaluation of differences in the expression of immune regulatory genes and immune checkpoint-associated genes between the high- and low-KIF18A groups.

Differential expression and enrichment analysis

Differential expression was analyzed using DESeq2 with the original gene-level count matrix from 291 TCGA-KIRP tumor samples dichotomized at the median KIF18A expression level into high- (n = 146) and low-expression (n = 145) groups [29]. *P* values were adjusted using the Benjamini-Hochberg procedure, and genes with an adjusted *P* value < 0.05 and an absolute |log2 fold change (FC)| > 1 were considered differentially expressed. Volcano plots were used to show the identified genes and a heatmap was created to show the patterns of expression of KIF18A and representative differentially expressed genes [30].

Functional enrichment analyses were conducted using the clusterProfiler package [31]. Gene

Ontology (GO) and Kyoto Encyclopedia of Genes and Genomes (KEGG) over-representation analyses used the 1,149 differentially expressed genes (DEGs) as the input list. The background universe comprised all genes annotated to the corresponding GO ontology (biological process, cellular component, or molecular function) or human KEGG pathway (hsa).

GSEA was conducted using the MSigDB Hallmark gene-set collection (h.all.v2026.1.Hs.symbols.gmt) [32]. Genes with available DESeq2 log2 FC values were ranked for the high- versus low-KIF18A comparison. Positive and negative normalized enrichment scores (NESs) indicate enrichment in the high- and low-KIF18A groups, respectively. The Z-score was calculated as (Nup - Ndown)/sqrt(Nterm).

Statistical analysis

All the statistical operations were done in R software. Independent two-group comparisons were assessed using two-sided Mann-Whitney U tests (Wilcoxon rank-sum tests). For clinicopathological variables with three or more categories, the Kruskal-Wallis test was first used for the overall comparison, followed by Dunn's post hoc test for pairwise comparisons. Tests were two-tailed, and $P < 0.05$ was considered to be statistically significant unless stated otherwise.

Results

KIF18A was upregulated in KIRP and showed diagnostic value

Pan-cancer expression analysis revealed dysregulated KIF18A expression across multiple tumor types. In the TCGA cohort, KIF18A was significantly upregulated in BLCA, BRCA, CESC, CHOL, COAD, ESCA, GBM, HNSC, KIRC, KIRP, LIHC, LUAD, LUSC, PCPG, READ, STAD, and UCEC compared with corresponding normal tissues (**Figure 1A**). After integrating TCGA and GTEx data, increased KIF18A expression was also observed in ACC, BLCA, BRCA, CESC, CHOL, COAD, DLBC, ESCA, GBM, HNSC, KIRC, KIRP, LGG, LIHC, LUAD, LUSC, OV, PAAD, PCPG, PRAD, READ, SKCM, STAD, THCA, THYM, UCEC, and UCS (**Figure 1B**).

In KIRP, KIF18A expression was higher in tumor tissues than in normal kidney tissues in both the unpaired TCGA analysis and the combined TCGA-GTEx analysis (**Figure 1C**, **1D**). Paired tumor-adjacent normal comparisons yielded the same expression trend (**Figure 1E**). ROC analysis comparing 291 KIRP tumors with 32 tumor-adjacent normal kidney samples in the TCGA cohort yielded an AUC of 0.693 (95% CI, 0.621-0.765), indicating modest tissue-level discrimination (**Figure 1F**). This estimate was derived from the analysis cohort and requires independent validation before clinical application.

High KIF18A expression was associated with poor prognosis in KIRP

Pan-cancer Cox regression analysis was used to assess the prognostic relevance of KIF18A. When modeled as a continuous variable, higher KIF18A expression was associated with unfavorable overall survival in ACC, KICH, KIRC, KIRP, LGG, LIHC, LUAD, MESO, PAAD, PCPG, SARC, and UVM, whereas a favorable association was observed in READ and THYM. Among these cancers, KIRP showed a marked prognostic association, with an HR of 4.127, a 95% CI of 2.784-6.119, and $P < 0.001$ (**Figure 2A**).

In KIRP, Kaplan-Meier analyses using endpoint-specific high- and low-expression groups defined by the minimum-*P*-value approach showed shorter overall survival, disease-specific survival, and progression-free interval in the KIF18A-high groups (**Figure 2B-D**). After exclusion of cases with missing survival-time or outcome-status data, the high/low group sizes were 74/216 for overall survival, 73/213 for disease-specific survival, and 93/196 for progression-free interval, respectively. Time-dependent ROC analysis yielded AUC values of 0.821, 0.825, and 0.748 for 1-, 3-, and 5-year survival prediction, respectively (**Figure 2E**). These results represent in-cohort estimates and require independent validation.

KIF18A expression was related to clinicopathological features

The relationship between KIF18A expression and clinicopathological characteristics was examined in KIRP. KIF18A expression was higher in patients aged ≤ 60 years than in those aged > 60 years and was also higher in female patients than in male patients (**Figure 3A**, **3B**). Its expression increased with advancing pathological stage (**Figure 3C**). Patients with T3-T4

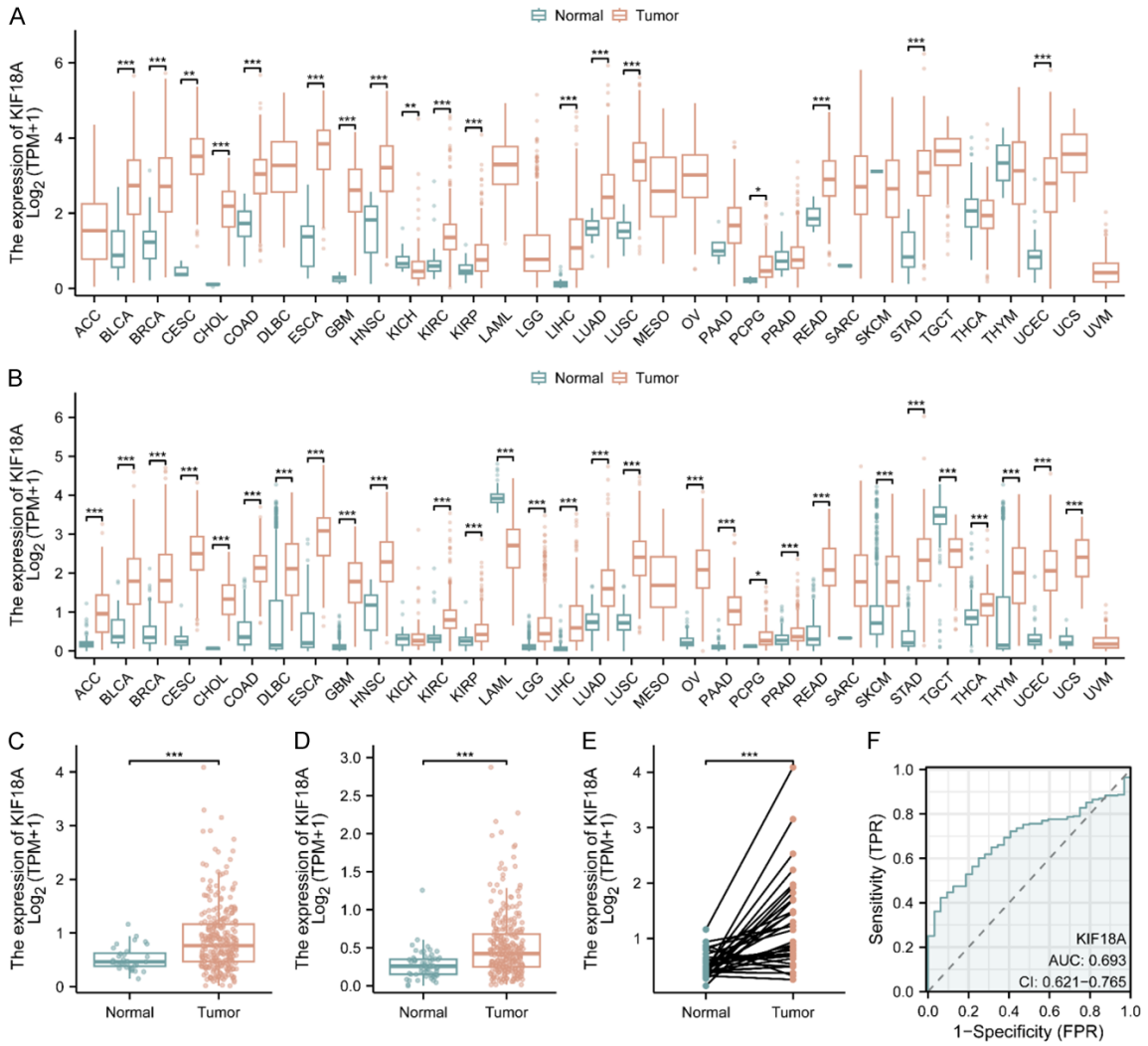


Figure 1. KIF18A expression pattern and diagnostic assessment in KIRP. A, B. Pan-cancer comparison of KIF18A expression based on TCGA and integrated TCGA-GTEx datasets. C, D. Differential expression of KIF18A between KIRP tumors and normal kidney tissues. E. Paired comparison of KIF18A expression between tumor tissues and matched adjacent normal tissues. F. ROC curve assessing tissue-level discrimination between 291 KIRP tumors and 32 tumor-adjacent normal kidney samples in the TCGA cohort. $^{*}P < 0.05$, $^{**}P < 0.01$, $^{***}P < 0.001$.

disease showed higher KIF18A expression than normal tissues and patients with lower T stages (**Figure 3D**). KIF18A expression was also increased in the N1-N2 group compared with the N0 group (**Figure 3E**) and in the M1 group compared with the M0 group (**Figure 3F**).

KIF18A expression was associated with immune infiltration

Immune infiltration analysis revealed significant differences in ssGSEA scores between the high- and low-KIF18A groups. Compared with the low-KIF18A group, the high-KIF18A group showed higher scores for activated dendritic cells (aDCs), T helper cells, central memory T cells (Tcm), and Th2 cells. In contrast, the high-KIF18A group showed lower scores for CD8 T cells, cytotoxic cells, dendritic cells (DCs), immature dendritic cells (iDCs), NK CD56-bright cells, macrophages, neutrophils, and Th17 cells (all $P < 0.05$; **Figure 4A**). Spearman correlation analysis showed positive correlations between KIF18A expression and T helper cells, Th2 cells, Tcm, and aDCs, whereas negative correlations were observed with DCs, iDCs, macrophages, Th17 cells, NK CD56bright cells, cytotoxic cells, neutrophils, CD8 T cells, B cells, and eosinophils (**Figure 4B**).

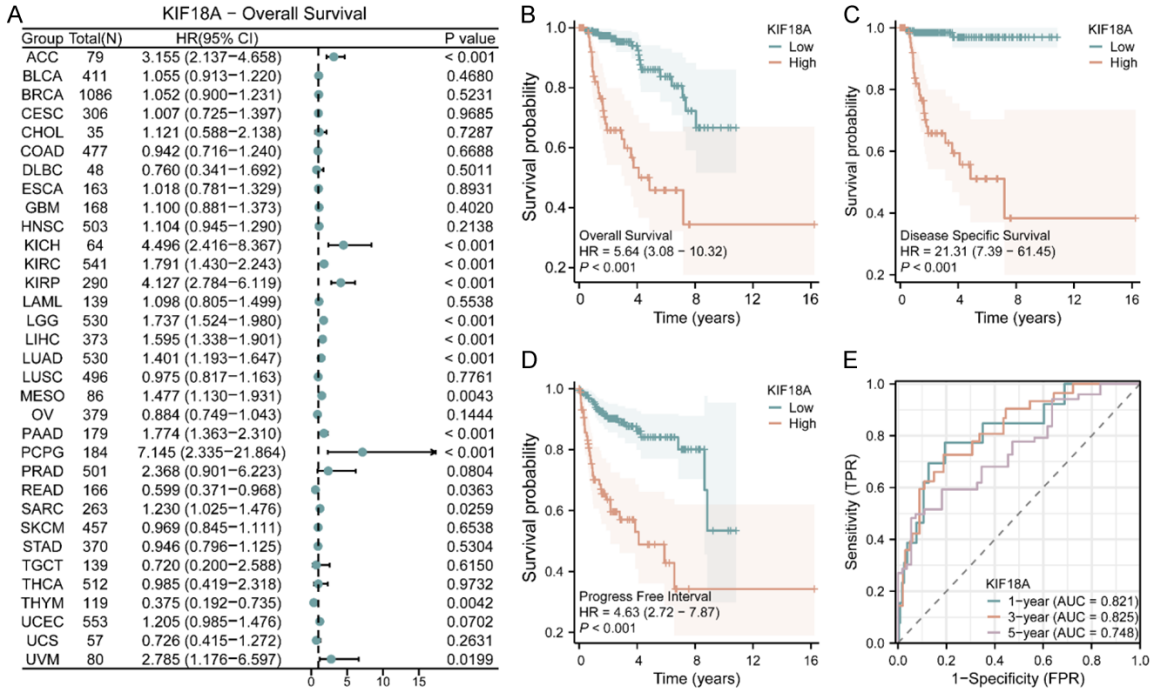


Figure 2. Association of KIF18A expression with survival outcomes in KIRP. A. Pan-cancer Cox regression analysis of continuous KIF18A expression and overall survival. B-D. Kaplan-Meier analyses of overall survival, disease-specific survival, and progression-free interval using endpoint-specific high- and low-expression groups defined by the minimum-*P*-value approach. E. Time-dependent ROC curves for predicting 1-, 3-, and 5-year overall survival in 290 KIRP patients with available OS time and status data; results represent in-cohort estimates.

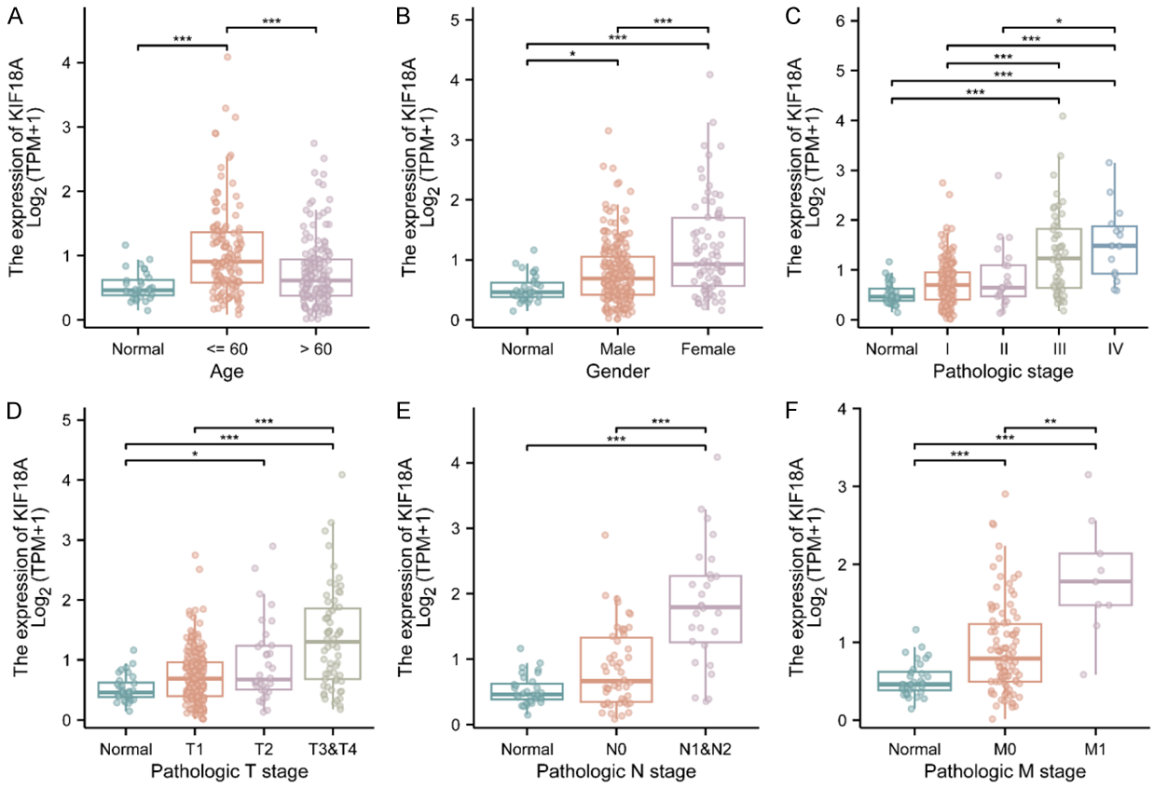


Figure 3. Distribution of KIF18A expression across clinicopathological subgroups in KIRP. A. Age-based subgroup comparison. B. Gender-based subgroup comparison. C. Pathological stage groups. D. T classification groups. E. N classification groups. F. M classification groups. $^{*}P < 0.05$, $^{**}P < 0.01$, $^{***}P < 0.001$.

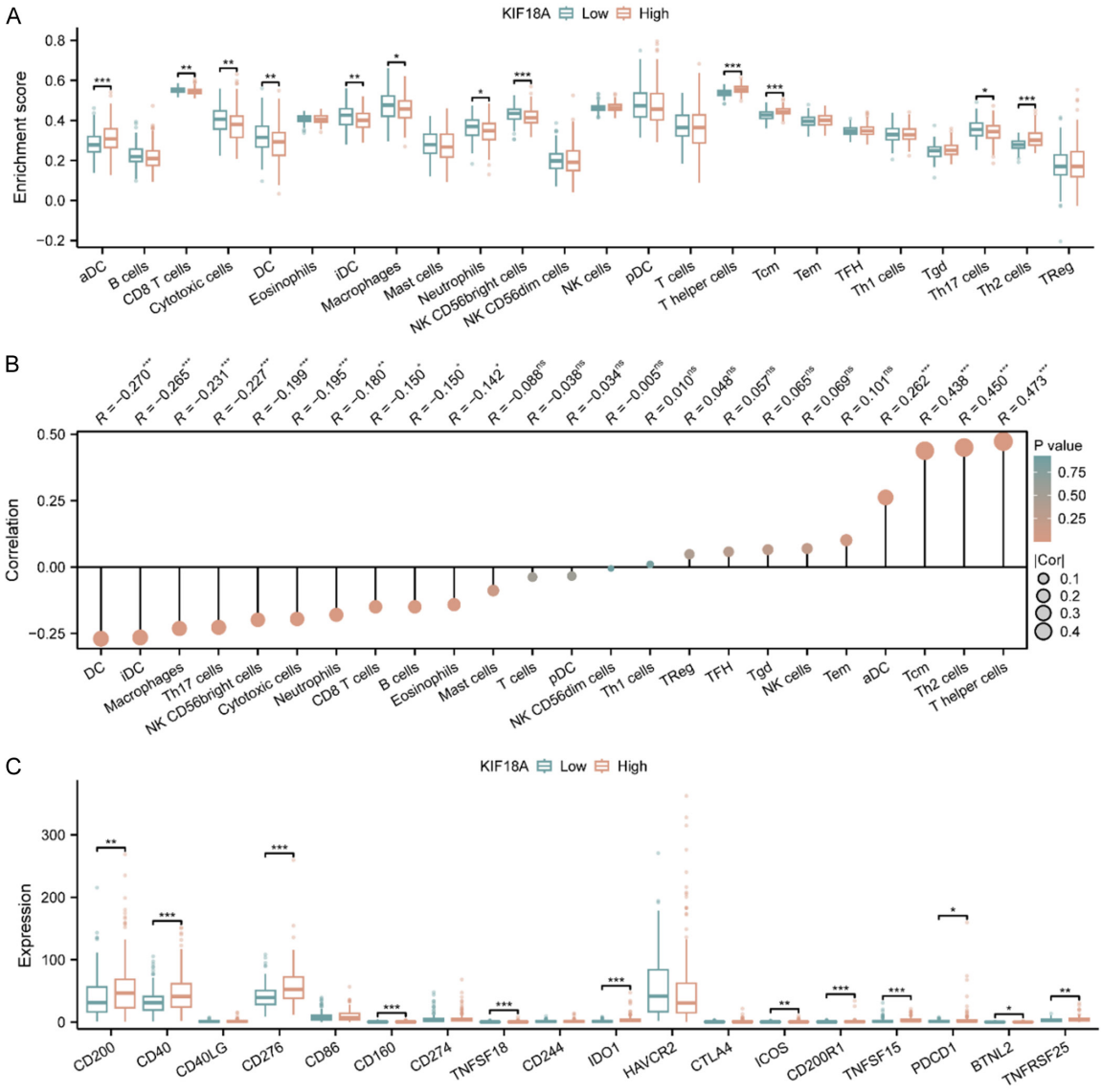


Figure 4. Immune characteristics associated with KIF18A expression in KIRP. A. Differences in immune-cell infiltration between KIF18A expression groups. B. Correlation between KIF18A expression and immune-cell infiltration patterns. C. Expression profiles of immune regulatory and checkpoint-related genes. *P < 0.05, **P < 0.01, ***P < 0.001.

The high-KIF18A expression group also showed increased expression of several immune regulatory and checkpoint-related genes, including CD200, CD40, CD276, CD160, TNFSF18, IDO1, ICOS, CD200R1, TNFSF15, PDCD1, BTNL2, and TNFRSF25 (**Figure 4C**).

Functional enrichment analysis of KIF18A-related genes

To explore biological features associated with KIF18A, KIRP samples were stratified into high- and low-expression groups. A total of 1,149 differentially expressed genes were identified using adjusted *P*-value < 0.05 and $|\log_2 FC| > 1$ as thresholds, including 896 upregulated and 253 downregulated genes (**Figure 5A**). Correlation analysis showed positive associations of KIF18A with ZIC2, ZIC5, MAGEC2, PAGE1, and CASP14, and negative associations with ABCB5 and ADGRG4 (**Figure 5B**).

GO and KEGG enrichment analyses showed that KIF18A-related genes were mainly enriched in cell division, chromosome segregation, nuclear division, sister chromatid segregation, ion channel complex, transmembrane trans-

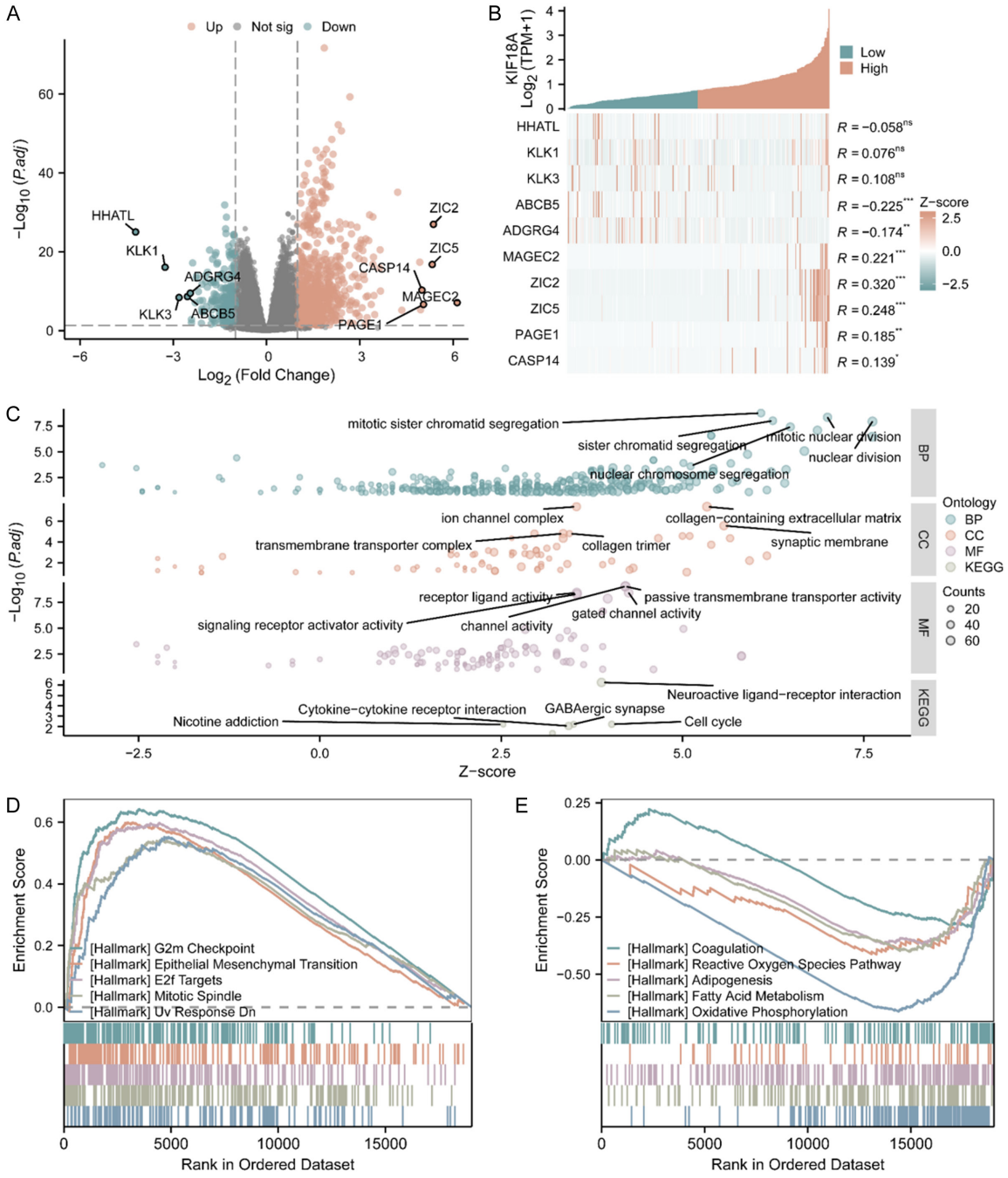


Figure 5. Differentially expressed genes and biological pathways related to KIF18A expression. (A) Identification of differentially expressed genes using volcano plots. (B) Heatmap showing co-expression patterns of KIF18A and representative differentially expressed genes. (C) GO and KEGG enrichment results. (D, E) GSEA results for pathways positively (D) and negatively (E) enriched in the high-KIF18A expression group.

porter complex, receptor ligand activity, channel activity, and cell cycle-related pathways. KEGG analysis also identified neuroactive ligand-receptor interaction, cytokine-cytokine receptor interaction, GABAergic synapse, and cell cycle pathways (**Figure 5C**; Table S1).

GSEA demonstrated positive enrichment of G2M checkpoint, epithelial-mesenchymal transition, E2F targets, mitotic spindle, and UV response DN pathways in the high-KIF18A expression group (**Figure 5D**; Table S2). By contrast, coagulation, the reactive oxygen spe-

cies pathway, adipogenesis, fatty acid metabolism, and oxidative phosphorylation were negatively enriched (**Figure 5E**).

Discussion

In this study, we systematically evaluated the expression pattern, clinicopathological relevance, immune associations, and potential biological functions of KIF18A in KIRP. KIF18A showed altered expression across multiple cancer types and was consistently upregulated in KIRP tumor tissues based on TCGA analysis, TCGA-GTEx integration, and paired tumor-adjacent normal tissue comparisons. ROC analysis indicated moderate diagnostic performance, suggesting that KIF18A may not be sufficient as a standalone diagnostic marker but could provide additional molecular information when combined with other diagnostic indicators.

Increased KIF18A expression correlated with reduced overall survival, disease-specific survival and progression-free interval in KIRP. Prognostic correlations of KIF18A have been reported earlier in renal cell carcinoma and pan-cancer cohorts [17, 19]. Moreover, the expression of KIF18A was positively correlated with pathological progression and was elevated in patients with advanced T stage, lymph node metastasis, and distant metastasis. These findings indicate that KIF18A expression can be indicative of a more aggressive biological condition in KIRP. Nonetheless, the question of whether KIF18A has independent prognostic value as compared to traditional clinicopathological variables needs to be addressed with the help of external cohorts and multivariate models.

The results of the enrichment analysis offer a potential reason behind the correlation between KIF18A expression and clinical outcomes. The genes associated with KIF18A were primarily involved in cell division, chromosome segregation, nuclear division, sister chromatid segregation and cell-cycle control. GSEA also revealed that tumors with high levels of KIF18A were enriched in G2/M checkpoint regulation, E2F target signatures, and mitotic spindle-related pathways. These results are consistent with the established role of KIF18A as a kinesin-8 motor protein that regulates kinetochore-microtubule interactions, chromosome congression and alignment of chromosomes during mitosis [16, 33]. Recent research has proposed that chromosomally unstable tumors can rely on KIF18A to preserve mitotic stability, and KIF18A inhibition can selectively disrupt this reliance [20, 21]. Specifically, Phillips et al. found that a selective KIF18A inhibitor had antitumor activity in cancer models with chromosomal instability, which pharmacologically supports the hypothesis that KIF18A-mediated regulation of mitosis can be therapeutically targeted [34]. Moreover, nano-delivery strategies using siRNA have also given additional impetus to the investigation of KIF18A-directed therapeutic strategies [35]. Thus, the upregulation of KIF18A in KIRP could reflect a tumor condition with increased proliferation and dependence on mitotic control, but this remains to be directly confirmed in KIRP models.

In addition to its involvement in cell-cycle regulation, the expression of KIF18A was also associated with EMT-related processes. EMT and epithelial-mesenchymal plasticity facilitate tumor-cell invasion, metastatic spread, and treatment resistance, thus facilitating aggressive cancer progression [36-38]. The enrichment of EMT in the current work was in line with the increased level of KIF18A in patients with advanced T stage, lymph node, and distant metastasis. Other experimental research has also shown that knockdown of KIF18A inhibits proliferation, migration and invasion in a variety of cancer models [18, 39, 40]. These findings prompt the hypothesis that KIF18A expression can be linked to proliferative and invasive characteristics of KIRP, but there is currently no direct evidence of this using KIRP-specific experimental systems.

The immune analyses further indicate that KIF18A is associated with changes in the KIRP immune microenvironment. The expression of KIF18A was positively correlated with T helper cells, Th2 cells, central memory T cells and activated dendritic cells but negatively correlated with CD8 T cells, cytotoxic cells, NK CD56bright cells, macrophages, neutrophils, B cells, eosinophils, and immature dendritic cells. The continuous correlation analysis indicated an inverse relationship between KIF18A expression and CD8 T-cell/cytotoxic-cell signatures, suggesting that increasing KIF18A levels may be associated with reduced cytotoxic immune characteristics. However, immune-cell

differences observed after dichotomizing samples into high- and low-KIF18A groups should be interpreted separately because cutoff-based comparisons may not fully reflect continuous expression trends. Moreover, several immune regulatory and checkpoint-related genes such as CD200, CD40, CD276, CD160, TNFSF18, IDO1, ICOS, CD200R1, TNFSF15, PDCD1, BTNL2, and TNFRSF25 were more highly expressed in the KIF18A-high subgroup. CD276/B7-H3 and IDO1 are known to control tumor immune escape and response to immunotherapy [41, 42]. Recent immuno-oncology experiments have also highlighted the need to alter immune responses in solid tumors [43]. Additionally, chromosomally unstable tumor model studies indicate that inhibition of KIF18A can lead to decreased tumor growth, affect antitumor immunity, and enhance PD-1 blockade responses [39]. However, the present results are obtained based on bulk RNA-sequencing data, and more single-cell, spatial transcriptomic, or multiplex immunofluorescence experiments are needed to characterize the cellular origin and spatial structure of these immune changes. Recent developments in single-cell RNA sequencing in tumor immunology also justify the necessity to address immune-cell heterogeneity and functional states at single-cell resolution when interpreting transcriptome-based immune infiltration outcomes [44].

These immune results are also in line with the general notion that cancer progression is driven by interactions between cancer cells and non-cancerous components of the tumor microenvironment. In renal cancer, cancer-associated fibroblasts have been shown to create an immunosuppressive environment through M2-like macrophage polarization, recruitment of regulatory T cells, extracellular matrix remodeling, and exclusion or dysfunction of cytotoxic T cells [8, 45, 46]. While this study did not directly assess stromal-cell populations, including fibroblasts, the associations between KIF18A expression, decreased cytotoxic immune signatures, and increased immune regulatory genes suggest that KIF18A-high KIRP may reflect a transcriptional state linked to immune microenvironment remodeling.

Metabolic pathway analysis revealed decreased enrichment of fatty acid metabolism, oxidative phosphorylation, adipogenesis and reactive oxygen species-related pathways in the KIF18A-high group. Metabolic remodeling is now known to be a key aspect of renal cell carcinoma, with changes in nutrient utilization, lipid metabolism, mitochondrial adaptation, and metabolic crosstalk between tumor cells and the tumor microenvironment able to drive tumor progression, reprogram immune regulation, and lead to therapeutic resistance [47, 48]. Thus, these alterations could represent a transition from differentiated metabolic activity to a more proliferative tumor state in KIRP. It is not clear whether KIF18A is involved in metabolic regulation or primarily reflects cell-cycle activation. Since oxidative phosphorylation can be dynamically regulated by tumor type, stage and microenvironment, the decreased oxidative phosphorylation signature in KIF18A-high tumors may be due to other metabolic reprogramming events rather than a direct role of KIF18A [49]. These metabolic results are in line with recent studies of renal cancer that demonstrate that post-translational modification-associated programs (such as palmitoylation and lactylation-associated signatures) are strongly associated with prognosis, immune microenvironment remodeling, and response to therapy or immunotherapy in clear cell renal cell carcinoma [10, 50]. A comprehensive study of palmitoylation in clear cell renal cell carcinoma demonstrated that palmitoylation-related signatures were linked to survival outcomes, genetic variations, single-cell expression profiles, cell-cell communication and immunotherapy-related characteristics [10]. While KIF18A itself is not a palmitoylation marker in this analysis, the negative enrichment of fatty acid metabolism and oxidative phosphorylation in KIF18A-high tumors indicates that KIF18A expression might be related to other metabolic and immune-related transcriptional changes in KIRP.

There are a number of limitations that should be taken into account. First, the analyses were based mostly on retrospective publicly available datasets and validation in independent KIRP cohorts was required. Even though TCGA-GTEx integration has enhanced the number of normal controls, there is no possibility of completely excluding possible batch effects between datasets. Second, the present analysis was mainly conducted based on transcrip-

tomic data, and protein-level confirmation using such methods as immunohistochemistry will be required to confirm the expression of KIF18A in KIRP tissues. Third, the bulk RNA-sequencing profiles were used to estimate immune infiltration, but future single-cell sequencing, spatial transcriptomics, or multiplex immune profiling could give a more detailed picture of the origin and localization of immune cells. Lastly, the existing findings explain relationships and not direct processes. The functional experiments of KIF18A knockdown, overexpression, and pharmacological inhibition in KIRP models will be significant in defining its role in tumor growth, invasion, immune control, and metabolic changes. If KIF18A is further established as a functional therapeutic target in KIRP, new functionalized exosome-based delivery systems can offer a possible platform for future KIF18A-directed nucleic acid or drug delivery strategies [51].

Conclusions

KIF18A was expressed more strongly in KIRP tumors and correlated with clinical outcome, tumor progression-related features, and immune-related features. Higher KIF18A expression was associated with worse survival, higher clinicopathological characteristics, variations in immune infiltration patterns, upregulation of immune regulatory and checkpoint-related genes, and enrichment of cell-cycle regulation, mitosis, EMT, and metabolism pathways.

Combined, these findings indicate a potential involvement of KIF18A in KIRP progression and suggest that its expression might be informative for prognosis and immune profiling. However, given that the current evidence is based mainly on public data, further experimental validation and confirmation in independent clinical cohorts are needed to determine the functional role and potential clinical value of KIF18A in KIRP.

Acknowledgements

This work was supported by the National Key R&D Program of China (Grants 2023YFC2705600 and 2023YFC2705602).

Disclosure of conflict of interest

None.

Address correspondence to: Dr. Yanqiu Zhang, SPH XingLing Sci. & Tech. Pharmaceutical Co., Ltd., Shanghai 201707, China. E-mail: yqiuzhang@163.com

References

[1] Cancer Genome Atlas Research Network; Linehan WM, Spellman PT, Ricketts CJ, Creighton CJ, Fei SS, Davis C, Wheeler DA, Murray BA, Schmidt L, Vocke CD, Peto M, Al Mamun AA, Shinbrot E, Sethi A, Brooks S, Rathmell WK, Brooks AN, Hoadley KA, Robertson AG, Brooks D, Bowlby R, Sadeghi S, Shen H, Weisenberger DJ, Bootwalla M, Baylin SB, Laird PW, Cherniack AD, Saksena G, Haake S, Li J, Liang H, Lu Y, Mills GB, Akbani R, Leiserson MD, Raphael BJ, Anur P, Bottaro D, Albiges L, Barnabas N, Choueiri TK, Czerniak B, Godwin AK, Hakimi AA, Ho TH, Hsieh J, Ittmann M, Kim WY, Krishnan B, Merino MJ, Mills Shaw KR, Reuter VE, Reznik E, Shelley CS, Shuch B, Signoretti S, Srinivasan R, Tamboli P, Thomas G, Tickoo S, Burnett K, Crain D, Gardner J, Lau K, Mallery D, Morris S, Paulauskis JD, Penny RJ, Shelton C, Shelton WT, Sherman M, Thompson E, Yena P, Avedon MT, Bowen J, Gastier-Foster JM, Gerken M, Leraas KM, Lichtenberg TM, Ramirez NC, Santos T, Wise L, Zmuda E, Demchok JA, Felau I, Hutter CM, Sheth M, Sofia HJ, Tarnuzzer R, Wang Z, Yang L, Zenklusen JC, Zhang J, Ayala B, Baboud J, Chudamani S, Liu J, Lolla L, Naresh R, Pihl T, Sun Q, Wan Y, Wu Y, Ally A, Balasundaram M, Balu S, Beroukhim R, Bodenheimer T, Buhay C, Butterfield YS, Carlsen R, Carter SL, Chao H, Chuah E, Clarke A, Covington KR, Dahdouli M, Dewal N, Dhalla N, Doddapaneni HV, Drummond JA, Gabriel SB, Gibbs RA, Guin R, Hale W, Hawes A, Hayes DN, Holt RA, Hoyle AP, Jefferys SR, Jones SJ, Jones CD, Kalra D, Kovar C, Lewis L, Li J, Ma Y, Marra MA, Mayo M, Meng S, Meyerson M, Mieczkowski PA, Moore RA, Morton D, Mose LE, Mungall AJ, Muzny D, Parker JS, Perou CM, Roach J, Schein JE, Schumacher SE, Shi Y, Simons JV, Sipahimalani P, Skelly T, Soloway MG, Sougnez C, Tam A, Tan D, Thiessen N, Veluvolu U, Wang M, Wilkerson MD, Wong T, Wu J, Xi L, Zhou J, Bedford J, Chen F, Fu Y, Gerstein M, Haussler D, Kasaian K, Lai P, Ling S, Radenbaugh A, Van Den Berg D, Weinstein JN, Zhu J, Albert M, Alexopoulou I, Andersen JJ, Auman JT, Bartlett J, Bastacky S, Bergsten J, Blute ML, Boice L, Bollag RJ, Boyd J, Castle E, Chen YB, Cheville JC, Curley E, Davies B, DeVolk A, Dhir R, Dike L, Eckman J, Engel J, Harr J, Hrebinko R, Huang M, Huelsenbeck-Dill L, Iacocca M, Jacobs B, Lobis M, Maranchie JK,

McMeekin S, Myers J, Nelson J, Parfitt J, Parwani A, Petrelli N, Rabeno B, Roy S, Salner AL, Slaton J, Stanton M, Thompson RH, Thorne L, Tucker K, Weinberger PM, Winemiller C, Zach LA and Zuna R. Comprehensive molecular characterization of papillary renal-cell carcinoma. N Engl J Med 2016; 374: 135-145.

[2] Al-Qudimat AR, Altahtamouni SB, Elaarag M, Singh K, Abdelrahman M, Khalil IA, Hasan SA, Al-Oweidat I and Aboumarzouk OM. Surgical strategies in renal cancer: a meta-analysis of partial vs. radical nephrectomy outcomes across tumor stages. Qatar Med J 2025; 2025: 54.

[3] Powles T, Albiges L, Bex A, Comperat E, Grünwald V, Kanesvaran R, Kitamura H, McKay R, Porta C, Procopio G, Schmidinger M, Suarez C, Teoh J, de Velasco G, Young M and Gillessen S; ESMO Guidelines Committee. Electronic address: clinicalguidelines@esmo.org. Renal cell carcinoma: ESMO Clinical Practice Guideline for diagnosis, treatment and follow-up. Ann Oncol 2024; 35: 692-706.

[4] Nepali PR, Eraky A, Okhawere KE, Dogra N, Mehrazin R, Badani K and Kyprianou N. Molecular and therapeutic landscape of non-clear cell renal carcinoma. Nat Rev Urol 2025; 22: 735-755.

[5] Chawla NS, Sayegh N, Prajapati S, Chan E, Pal SK and Chehrazi-Raffle A. An update on the treatment of papillary renal cell carcinoma. Cancers (Basel) 2023; 15: 565.

[6] Marchioni M, Rivas JG, Autran A, Socarras M, Albisinni S, Ferro M, Schips L, Scarpa RM, Papalia R and Esperto F. Biomarkers for renal cell carcinoma recurrence: state of the art. Curr Urol Rep 2021; 22: 31.

[7] Liu JF, Xia J, Rich J, Zhao S, Yang K, Lu B, Chen Y, Ye TW and Huang TJ. An acoustofluidic device for sample preparation and detection of small extracellular vesicles. Cyborg Bionic Syst 2025; 6: 0319.

[8] Wang M, Zhao Y, Xu K, Liu C, Zhong H, Wu Y, Zhang K and Wei S. Cancer-associated fibroblasts in clear cell renal cell carcinoma: functional heterogeneity, tumor microenvironment crosstalk, and therapeutic opportunities. Front Immunol 2025; 16: 1617968.

[9] McKinnon MB, Rini BI and Haake SM. Biomarker-informed care for patients with renal cell carcinoma. Nat Cancer 2025; 6: 573-583.

[10] Zhang D, Zhang K, Deng M, Ma J, Zhu J, Shen S, Xie J and Chen C. Integrated genomic and functional characterization of palmitoylation in clear cell renal cell carcinoma. Hum Mutat 2025; 2025: 4647115.

[11] Fan B, Zhang J, Li C and Zhang X. New trend in molecular diagnostics: insights from the tumor microenvironment. Interdisciplinary Medicine 2025; 3: e70048.

[12] Hanahan D. Hallmarks of cancer: new dimensions. Cancer Discov 2022; 12: 31-46.

[13] Matthews HK, Bertoli C and de Bruin RAM. Cell cycle control in cancer. Nat Rev Mol Cell Biol 2022; 23: 74-88.

[14] Bakhoum SF and Cantley LC. The multifaceted role of chromosomal instability in cancer and its microenvironment. Cell 2018; 174: 1347-1360.

[15] Hirokawa N, Noda Y, Tanaka Y and Niwa S. Kinesin superfamily motor proteins and intracellular transport. Nat Rev Mol Cell Biol 2009; 10: 682-696.

[16] Stumpff J, von Dassow G, Wagenbach M, Asbury C and Wordeman L. The kinesin-8 motor Kif18A suppresses kinetochore movements to control mitotic chromosome alignment. Dev Cell 2008; 14: 252-262.

[17] Chen QI, Cao B, Nan N, Wang YU, Zhai XU, Li Y and Chong T. Elevated expression of KIF18A enhances cell proliferation and predicts poor survival in human clear cell renal carcinoma. Exp Ther Med 2016; 12: 377-383.

[18] Qian LX, Cao X, Du MY, Ma CX, Zhu HM, Peng Y, Hu XY, He X and Yin L. KIF18A knockdown reduces proliferation, migration, invasion and enhances radiosensitivity of esophageal cancer. Biochem Biophys Res Commun 2021; 557: 192-198.

[19] Liu T, Yang K, Chen J, Qi L, Zhou X and Wang P. Comprehensive pan-cancer analysis of KIF18A as a marker for prognosis and immunity. Biomolecules 2023; 13: 326.

[20] Marquis C, Fonseca CL, Queen KA, Wood L, Vandal SE, Malaby HLH, Clayton JE and Stumpff J. Chromosomally unstable tumor cells specifically require KIF18A for proliferation. Nat Commun 2021; 12: 1213.

[21] Payton M, Belmontes B, Hanestad K, Moriguchi J, Chen K, McCarter JD, Chung G, Ninniri MS, Sun J, Manoukian R, Chambers S, Ho SM, Kurzeja RJM, Edson KZ, Dahal UP, Wu T, Wannberg S, Beltran PJ, Canon J, Boghossian AS, Rees MG, Ronan MM, Roth JA, Minocherhomji S, Bourbeau MP, Allen JR, Coxon A, Tamayo NA and Hughes PE. Small-molecule inhibition of kinesin KIF18A reveals a mitotic vulnerability enriched in chromosomally unstable cancers. Nat Cancer 2024; 5: 66-84.

[22] Zhang B, Wang F, Huang H, Zhong X, Chen Q, Liu X and Nair S. Tumor microenvironment characterization identifies KIF15 as an immunosuppressive driver in breast cancer. Hum Mutat 2026; 2026: 8861116.

[23] Jiang H, Niu W, Pan Y, Jiang Z, Wu J, Qiao Z, Jiang X and Huang L. Prognostic and immuno-

logical significance of TIPARP in pancreatic cancer. Dig Dis Sci 2026; 71: 1873-1888.
[24] GTEx Consortium. The GTEx Consortium atlas of genetic regulatory effects across human tissues. Science 2020; 369: 1318-1330.
[25] Vivian J, Rao AA, Nothaft FA, Ketchum C, Armstrong J, Novak A, Pfeil J, Narkizian J, Deran AD, Musselman-Brown A, Schmidt H, Amstutz P, Craft B, Goldman M, Rosenbloom K, Cline M, O'Connor B, Hanna M, Birger C, Kent WJ, Patterson DA, Joseph AD, Zhu J, Zaranek S, Getz G, Haussler D and Paten B. Toil enables reproducible, open source, big biomedical data analyses. Nat Biotechnol 2017; 35: 314-316.
[26] Blanche P, Dartigues JF and Jacqmin-Gadda H. Estimating and comparing time-dependent areas under receiver operating characteristic curves for censored event times with competing risks. Stat Med 2013; 32: 5381-5397.
[27] Zhou T, Zhang Y, Cao J, Tang Q, Liang Y, Zhang S, Hu M, Feng B and Jin J. Identification of immune infiltration-related ZNF480 for predicting prognosis in breast cancer. Am J Clin Exp Immunol 2025; 14: 1-13.
[28] Lin J, Wang J, Zhao J, Wu X, Hao L, Tan X, Yang L, Wu LL, Xia Y, Zhang X, Zhao K and Liu Y. Anoikis-related gene signature associates with the immune infiltration and predicts the prognosis of glioma patients. Genes Dis 2025; 12: 101346
[29] Love MI, Huber W and Anders S. Moderated estimation of fold change and dispersion for RNA-seq data with DESeq2. Genome Biol 2014; 15: 550.
[30] Tu L, Luo J, Yin Y and Yu H. Bioinformatics analysis across pan-cancer and experimental validation in hepatocellular carcinoma revealed the oncogenic role of SF3B6. Front Pharmacol 2025; 16: 1516534.
[31] Yu G, Wang LG, Han Y and He QY. clusterProfiler: an R package for comparing biological themes among gene clusters. OMICS 2012; 16: 284-287.
[32] Liberzon A, Birger C, Thorvaldsdóttir H, Ghandi M, Mesirov JP and Tamayo P. The Molecular Signatures Database (MSigDB) hallmark gene set collection. Cell Syst 2015; 1: 417-425.
[33] Du Y, English CA and Ohi R. The kinesin-8 Kif18A dampens microtubule plus-end dynamics. Curr Biol 2010; 20: 374-380.
[34] Phillips AF, Zhang R, Jaffe M, Schulz R, Carty MC, Verma A, Feinberg TY, Arensman MD, Chiu A, Letso R, Bosco N, Queen KA, Racela AR, Stumpff J, Andreu-Agullo C, Bettigole SE, Depetris RS, Drutman S, Su SM, Cogan DA and Eng CH. Targeting chromosomally unstable tumors with a selective KIF18A inhibitor. Nat Commun 2025; 16: 307.
[35] Aleixo DT, Cruz-Cazarim ELC, Ferreira KCB, Grossi LN, Braz WR, Silva NP, Pittella-Silva F, Dias MF, Fialho SL, Tavares GD and Pittella F. Breakthroughs in the nanoparticle-mediated delivery of siRNA for breast cancer treatment. Nanomedicine (Lond) 2025; 20: 2765-2789.
[36] Thompson EW, Redfern AD, Brabletz S, Berx G, Agarwal V, Ganesh K, Huang RY, Ishay-Ronen D, Savagner P, Sheng G, Stemmler MP and Brabletz T. EMT and cancer: what clinicians should know. Nat Rev Clin Oncol 2025; 22: 711-733.
[37] Allgayer H, Mahapatra S, Mishra B, Swain B, Saha S, Khanra S, Kumari K, Panda VK, Malhotra D, Patil NS, Leupold JH and Kundu GC. Epithelial-to-mesenchymal transition (EMT) and cancer metastasis: the status quo of methods and experimental models 2025. Mol Cancer 2025; 24: 167.
[38] Pastushenko I and Blanpain C. EMT transition states during tumor progression and metastasis. Trends Cell Biol 2019; 29: 212-226.
[39] Liu G, Zhang Y, Cao Z and Zhao Z. Targeting KIF18A triggers antitumor immunity and enhances efficiency of PD-1 blockade in colorectal cancer with chromosomal instability phenotype. Cell Death Discov 2025; 11: 130.
[40] Tanasuka P, Thongpon P, Chomwong S, Kongsintaweesuk S, Pinlaor S, Pongking T, Watcharadetwittaya S, Pairojkul C and Intuyod K. Suppression of kinesin family member-18A diminishes progression and induces apoptotic cell death of gemcitabine-resistant cholangiocarcinoma cells by modulating PI3K/Akt/mTOR and NF-κB pathways. PLoS One 2025; 20: e0334147.
[41] Zhou WT and Jin WL. B7-H3/CD276: an emerging cancer immunotherapy. Front Immunol 2021; 12: 701006.
[42] Fujiwara Y, Kato S, Nesline MK, Conroy JM, DePietro P, Pabla S and Kurzrock R. Indoleamine 2,3-dioxygenase (IDO) inhibitors and cancer immunotherapy. Cancer Treat Rev 2022; 110: 102461.
[43] Chen L, Li H, Liu J, Wang Y and Zhang S. Hollow mesoporous carbon nanospheres derived from metal-organic frameworks for efficient sono-immunotherapy against pancreatic cancer. Cyborg Bionic Syst 2025; 6: 0247.
[44] Liu Y, Yu X, Han Z, Wei Q, Niu Q, Yang C, Li JP, Guo Z and Zhang H. Advanced single-cell RNA sequencing in tumor immunology. Interdisciplinary Medicine 2025; 3: e20250060.
[45] Wen H, Zheng S, Zhu X, Wang L and Chen D. Characteristics of the tumor microenvironment and potential immunotherapy strategies in renal cell carcinoma. Front Immunol 2025; 16: 1643533.
[46] Luo J, Xiang X, Gong G and Jiang L. Cancer-associated fibroblast-mediated immune eva-

sion: molecular mechanisms of stromal-immune crosstalk in the tumor microenvironment. Front Immunol 2025; 16: 1617662.
[47] Zhang Y, Zhang S, Sun H and Xu L. The pathogenesis and therapeutic implications of metabolic reprogramming in renal cell carcinoma. Cell Death Discov 2025; 11: 186.
[48] Miao D, Shi J, Tan D, Zhao C, Lv Q, Lu F, Yang J, Yang H, Xiong Z and Zhang X. Targeting MMA-induced USP36 methylmalonylation to suppress macrophage polarization and tumor progression in clear-cell renal cell carcinoma. Cell Death Differ 2026; 33: 1648-1666.
[49] Chen K, Wang B, Shu H, Lyu J, Cui W and Fang H. Oxidative phosphorylation at the crossroads of cancer: metabolic orchestration, stromal collusion, and emerging therapeutic horizons. Interdisciplinary Medicine 2025; 3: e70054.
[50] Li Z, Li X, Hu S, Jiang S and Wang J. Integrative multi-omics analysis identifies a PTM-related immune signature and IRF9 as a driver in ccRCC. Front Immunol 2025; 16: 1707375.
[51] Deng R, Wei R, Peng X, Wang Q, Zhu T, Hu W, Dong W, Lu Y, Dong X, Liu Z, Yao F, Shu X, Fan J, Qiao L, Liang Y, Zhu Y and Zheng Q. Functionalized exosomes as emerging therapeutics for osteoarthritis: recent advances in their diverse cellular origins and effective targeted delivery. Genes Dis 2026; 102357.

Table S1. GO and KEGG over-representation analysis of differentially expressed genes between high- and low-KIF18A expression groups in KIRP

Ontology	Term ID	Gene set/pathway	GeneRatio	BgRatio	Adjusted *P* value (P.adjust)	FDR q value	Count	Z score
BP	GO:0000070	mitotic sister chromatid segregation	37/1023	171/18800	1.772E-09	1.526E-09	37	6.083
BP	GO:0140014	mitotic nuclear division	49/1023	293/18800	4.565E-09	3.931E-09	49	7.000
BP	GO:0000819	sister chromatid segregation	39/1023	205/18800	9.934E-09	8.555E-09	39	6.245
BP	GO:0000280	nuclear division	62/1023	446/18800	1.171E-08	1.009E-08	62	7.620
BP	GO:0098813	nuclear chromosome segregation	46/1023	287/18800	3.944E-08	3.397E-08	46	6.487
CC	GO:0062023	collagen-containing extracellular matrix	59/1083	429/19594	3.791E-08	3.196E-08	59	5.338
CC	GO:0034702	ion channel complex	46/1083	294/19594	3.791E-08	3.196E-08	46	3.539
CC	GO:0097060	synaptic membrane	49/1083	373/19594	2.644E-06	2.232E-06	49	5.571
CC	GO:1902495	transmembrane transporter complex	47/1083	377/19594	1.520E-05	1.283E-05	47	3.355
CC	GO:0005581	collagen trimer	19/1083	86/19594	1.520E-05	1.283E-05	19	3.441
MF	GO:0015267	channel activity	69/1043	489/18410	8.961E-10	7.715E-10	69	4.214
MF	GO:0022803	passive transmembrane transporter activity	69/1043	490/18410	8.961E-10	7.715E-10	69	4.214
MF	GO:0048018	receptor ligand activity	67/1043	489/18410	3.720E-09	3.204E-09	67	3.543
MF	GO:0022836	gated channel activity	53/1043	340/18410	3.720E-09	3.204E-09	53	4.258
MF	GO:0030546	signaling receptor activator activity	67/1043	496/18410	5.008E-09	4.313E-09	67	3.543
KEGG	hsa04080	Neuroactive ligand-receptor interaction	52/487	362/8164	5.491E-07	5.279E-07	52	3.883
KEGG	hsa04110	Cell cycle	20/487	126/8164	6.155E-03	5.917E-03	20	4.025
KEGG	hsa04727	GABAergic synapse	16/487	89/8164	6.155E-03	5.917E-03	16	3.500
KEGG	hsa05033	Nicotine addiction	10/487	40/8164	6.512E-03	6.261E-03	10	2.530
KEGG	hsa04060	Cytokine-cytokine receptor interaction	34/487	295/8164	9.096E-03	8.745E-03	34	3.430

Table S2. Hallmark gene-set enrichment analysis comparing high- and low-KIF18A expression groups in KIRP

Gene set	NES	Adjusted *P* value (p.adjust)	FDR q value	Enrichment direction
G2/M Checkpoint	2.451	1.250E-09	6.053E-10	Positive NES
Epithelial Mesenchymal Transition	2.286	1.250E-09	6.053E-10	Positive NES
E2F Targets	2.281	1.250E-09	6.053E-10	Positive NES
Mitotic Spindle	2.070	3.781E-09	1.831E-09	Positive NES
UV Response DN	2.035	2.616E-07	1.267E-07	Positive NES
Coagulation	-1.376	5.332E-02	2.582E-02	Negative NES
Reactive Oxygen Species Pathway	-1.602	2.649E-02	1.283E-02	Negative NES
Adipogenesis	-1.837	1.121E-05	5.427E-06	Negative NES
Fatty Acid Metabolism	-1.922	6.834E-06	3.309E-06	Negative NES
Oxidative Phosphorylation	-3.308	1.250E-09	6.053E-10	Negative NES